Modelling a buffered impact damper system using a spring-damper model of impact

Kuinian Li, Antony P Darby

Modelling a buffered impact damper system using a spring–damper model of impact

Kuinian Li[1] and Antony P. Darby[2]

[1] *Faculty of Engineering and the Environment, University of the Witwatersrand, Johannesburg, South Africa*
[2] *Department of Architecture and Civil Engineering, University of Bath, Bath, BA2 7AY, U.K.*

This paper presents a simple, practical method of modelling non-destructive impacts macroscopically, where the impact force and post-impact motion of the impacting bodies are of primary concern. The main focus is use of the model for simulating the dynamics of impact dampers used to control the response complex structures. A spring–damper pair is used to model the contact surface between the damper mass and the structure. The key to such a model is the ability to define the contact surface spring stiffness and damping parameters, which does not relate to simple mechanical properties under high-rate loading. A method is developed to derive these parameters by making use of experimentally measured coefficient of restitution and contact time of an impact. The model is able to represent contact force and elastic deformation during an impact process. A simple structure, controlled by an impact damper, is used to compare theoretical and experimental results and demonstrate the validity of the resulting spring–damper model. The results demonstrate that the spring–damper model can be effectively used in situations where the impulse–momentum model fails.

KEY WORDS: passive damping; impact; impulsive loads; structural dynamics

1. INTRODUCTION

An impact damper is a freely moving mass, constrained by stops fixed to a dynamically excited structure to be controlled. On impact with the stops, momentum is exchanged with the impact mass and energy is dissipated. A new type of impact damper, a buffered impact damper (BID), has been developed and investigated by Li and Darby [1]. It has been demonstrated that, compared with a conventional rigid impact damper, a BID not only significantly reduces the contact force and the associated high accelerations and noise caused by collisions but also

enhances the vibration control effect, which makes it ideal for many engineering applications. These beneficial effects result from the introduction of the buffer, which changes the contact characteristics of impact significantly. Experimental investigations [1] reveal that, dependent upon the buffer stiffness, the contact time of impact of a BID may be of the order of 100 times longer than that of a conventional rigid impact damper, with an associated peak contact force of the order of $\frac{1}{100}$ of that without a buffer. The modelling of the contact behaviour of a BID is the motivation for the research presented in this paper. This impact model must be able to satisfactorily represent both impact force and post-impact velocity.

There are several methods of modelling impacts macroscopically. One such macroscopic model of impact is the impulse–momentum model, which is employed in almost all published cases of modelling impact dampers (e.g. [2, 3]). The model assumes that the impact bodies are perfectly rigid and, therefore, does not account for any deformation of the bodies during impact. Consequently, the contact time of impact is assumed to be zero. The model governs the impact process via the law of conservation of momentum in addition to the relationship between the velocities before and after the impact, which is given by the coefficient of restitution. The major advantage of this model lies in its mathematical simplicity. However, it cannot represent the actual impact force and, furthermore, if the collision occurs between two flexible objects (as in the case of the BID), the contact time is not negligible, and therefore the model will fail to represent the impact behaviour satisfactorily.

A second macroscopic model of impact is the elastic, or Hertz, model of contact which allows for elastic deformation of a body during impact to occur [4]. However, this model does not allow for normal energy dissipation, i.e. impact is assumed to be perfectly elastic, giving a coefficient of restitution of unity.

A more appropriate method for a BID system is a combination of the above two methods, i.e. a combination of elastic deformation and energy dissipation. A possible way of achieving this is to model the impact as the compression of a spring and damper in parallel acting between the two impacting bodies and perpendicular to the plane of impact [5–7]. This is the so-called spring–damper model of impact. Given appropriate model parameters, it can represent overall impact behaviour very accurately, in terms of both contact force and post-impact velocity. The difficulty in implementing the model lies in establishing the parameters *a priori* [8]. Under high-rate loading, of the type caused by impact processes, the stiffness and damping parameters are not directly measurable. In making use of the spring–damper model for an impact process, investigators have tended to establish the parameters by trial and error, resulting only in a rough order of magnitude approximation [9]. To find the damping and stiffness parameters, a relationship with two other directly measurable parameters may be used. Masri [5] identified the dependence of the coefficient of restitution and contact time on the stiffness and damping parameters. This paper aims at making use of these more easily measured parameters to calculate the stiffness and damping parameters. While this does not provide parameters *a priori*, it does allow the parameters to be found using simple, practical measurements in isolation and then applied to more complex impact systems, such as a BID.

2. THE SPRING–DAMPER MODEL OF IMPACT

A spring–damper pair is employed to model the impact surface of two impact bodies, m_1 and m_2, as shown in Figure 1. The parameters of the spring–damper model, the spring stiffness, k_b,

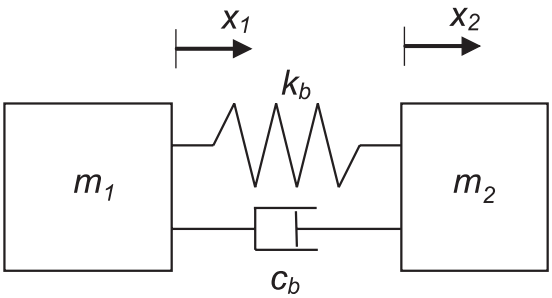

Figure 1. Model of an impact pair.

and the damping, c_b, are to be determined. It is assumed that the coefficient of restitution, e, and contact time of collision, T_c, can be measured. Referring to Figure 1, the dynamics of the two masses during contact can be represented by the following differential equations:

$$m_2\ddot{x}_2 + c_b(\dot{x}_2 - \dot{x}_1) + k_b(x_2 - x_1) = 0 \tag{1}$$

$$m_1\ddot{x}_1 + c_b(\dot{x}_1 - \dot{x}_2) + k_b(x_1 - x_2) = 0 \tag{2}$$

These can be rewritten in terms of relative displacement, $y = x_2 - x_1$, as

$$\ddot{y} + 2\zeta\omega_n\dot{y} + \omega_n y = 0 \tag{3}$$

where

$$\omega_n = \sqrt{\frac{k_b}{m_2}(1+\mu)} \quad \text{and} \quad \mu = \frac{m_2}{m_1}$$

and

$$\zeta = \frac{c_b}{2\omega_n m_2}(1+\mu) = \frac{c_b\sqrt{1+\mu}}{2\sqrt{k_b m_2}} \tag{4}$$

Assuming initial conditions $t = 0$, $y = 0$, and $\dot{y} = \dot{y}_0$, the displacement response is given as

$$y = \frac{\dot{y}_0}{\omega}\exp(-\zeta\omega_n t)\sin\omega t \tag{5}$$

and in terms of relative velocity it is given as

$$\dot{y} = \frac{\dot{y}_0}{\omega}\exp(-\zeta\omega_n t)(\omega\cos\omega t - \zeta\omega_n\sin\omega t) \tag{6}$$

where $\omega = \omega_n\sqrt{1-\zeta^2}$ is the damped natural frequency. At the end of the collision process, the end conditions are $t = T_c$, $y = 0$, and, $\dot{y} = e\dot{y}_0$, where e is the coefficient of restitution of the collision and T_c the duration of the collision (the contact time). Equation (5) satisfies these end conditions when $\omega T_c = \omega_n\sqrt{1-\zeta^2}T_c = \pi$. Using this and the end conditions, the following relationship is formed:

$$e\dot{y}_0 = \frac{\dot{y}_0}{\omega}\exp(-\zeta\omega_n T_c)(-\omega) = -\dot{y}_0\exp(-\zeta\omega_n T_c) \tag{7}$$

Given that $\dot{y}_0 \neq 0$ (otherwise no collision occurs), Equation (7) can be rearranged to give

$$\zeta \omega_n T_c = -\ln(e) \tag{8}$$

This gives a relationship between the damping ratio, the contact time, and the coefficient of restitution. Thus, substituting Equation (4) into Equation (8) yields a value for the damping:

$$c_b = \frac{2m_2 \ln(e)}{(1+\mu)T_c} \tag{9}$$

Similarly, the stiffness parameter can be obtained as

$$k_b = \frac{m_2}{(1+\mu)T_c^2}(\pi^2 + (\ln(e))^2) \tag{10}$$

From Equations (9) and (10) it can be seen that k_b and c_b are related to both the coefficient of restitution and the contact time, T_c, allowing realistic modelling of elastic impact behaviour. In the limiting case where $T_c \to 0$, then $k_b \to \infty$ and $c_b \to \infty$, implying, as would be expected, a rigid body collision, which might be adequately represented by the impulse–momentum model. Similarly, if the coefficient of restitution $e = 1$ (implying no energy loss during impact), then from Equation (9) it can be seen that $c_b = 0$, as would be expected.

It should be noted that it is assumed in the derivation of Equations (9) and (10) that k_b and c_b remain constant for the duration of a collision. It is widely accepted that both the coefficient of restitution e and the contact time T_c may, to some degree, depend on the impact velocity, $\dot{y}_0$; therefore, the values of k_b and c_b may vary accordingly for a given impact but can be assumed to remain constant during the impact itself. This impact velocity dependence of k_b and c_b would be simple to implement in an impact system model using the equations derived above, although it has been found to be unnecessary for the problems investigated in this paper. Examples of measured coefficient of restitution and contact time, together with the calculated damping and stiffness of the impact process, are given in Table I for various buffer materials.

3. COMPARISON BETWEEN EXPERIMENTAL RESULTS AND NUMERICAL SIMULATIONS

A series of experiments have been performed to compare the spring–damper model with the impulse–momentum model for impact. As the driving force for this work, the system chosen for the experiments is a single-degree-of-freedom (SDOF) system equipped with an impact damper allowing reliable comparison to be made with simulated results. The SDOF primary structure is a single-storey shear frame, as shown in Figure 2 together with an impact damper mass. The beam of the SDOF structure is a 40×30 mm cross-section aluminium alloy beam of mass $M = 1.35$ kg. The lateral stiffness of the two 40×1 mm cross-section steel columns is $K = 865$ N/m, obtained by static load-deflection tests, and damping $C = 2 \times \xi \times \sqrt{K/M} = 1.092$ N s/m, obtained from an experimentally derived transfer function. The natural frequency of this system is approximately 4.0 Hz. The impact mass is a steel ball of 30 mm diameter and mass $m = 0.11$ kg, giving a mass ratio (i.e. m/M) of $\mu = 0.082$. The total clearance between the mass and the stops, referring to Figure 2, is $d = d_1 + d_2 = 15$ mm. The lateral response of the structure was measured using an accelerometer fixed to mass M.

Experimental results using both a conventional rigid impact damper (where the impact mass is steel and the stops are of aluminium alloy) and a BID are employed. The buffer consisted of

a flexible sponge material, referred to as buffer 1 in Table I. Numerical simulations employing both the spring–damper model and the impulse–momentum model of impact are performed and the results are compared with the equivalent experimental results. Free vibration tests simulate the response of the structure to a transient load (such as wind gust loading), whereas random forced base excitation is used to simulate seismic excitation. The free vibration tests are provided to clearly demonstrate the underlying characteristics of the two impact models for a simple load–response relationship. The random forced vibration tests result in a response over a wide frequency range, rather than just at the natural frequency. This demonstrates the applicability of the model for more complex interaction between the structural motion and the motion of the impact mass, where impacts occur at many different velocities. This is a case that could not be modelled except via a non-linear numerical method, incorporating a suitable impact model.

Coefficients of restitution were measured using a drop test, i.e. the impact mass was dropped from various predetermined heights and the rebound height measured. The pre- and post-impact velocities could then be calculated and, hence, the coefficient of restitution is established. The contact time, T_c, was measured from the time history of contact force measured using a force transducer fixed to the underside of the buffer material. For the experimental investigations described in this paper, the impact velocity range varies between approximately 0.15 and 1.0 m/s. The contact time over this range remains approximately constant for each material as indicated by the experimental results shown in Figure 3. Similarly, the coefficients of restitution remained approximately constant. Therefore, the effect of impact velocity on both the contact time and the coefficient of restitution is neglected and average values are used.

The average coefficient of restitution for the conventional impact damper was $e = 0.46$, whereas for the BID $e = 0.61$. For the conventional impact damper, $T_c = 0.0003$ s, whereas for

Table I. Measured impact surface parameters.

Impact mass	Buffer/stop material	e	T_c (s)	k_b (kN/m)	c_b (N m/s)
Steel ball	Buffer 1 (sponge)	0.61	0.025	1.65	4.05
Steel ball	Buffer 2 (soft rubber)	0.44	0.019	2.99	8.80
Steel ball	Buffer 3 (hard rubber)	0.53	0.004	65.7	32.5
Steel ball	Buffer 4 (hard acrylic)	0.49	0.003	118.0	48.7
Steel ball	No buffer (Al alloy)	0.46	0.0003	11 900.0	530

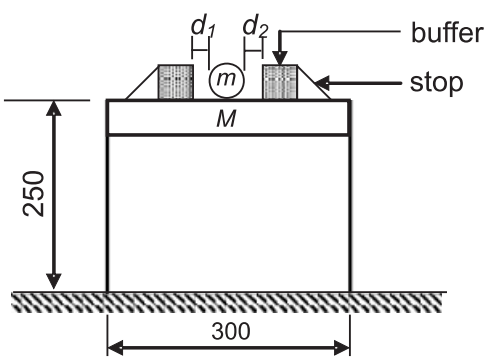

Figure 2. Experimental model—SDOF structure.

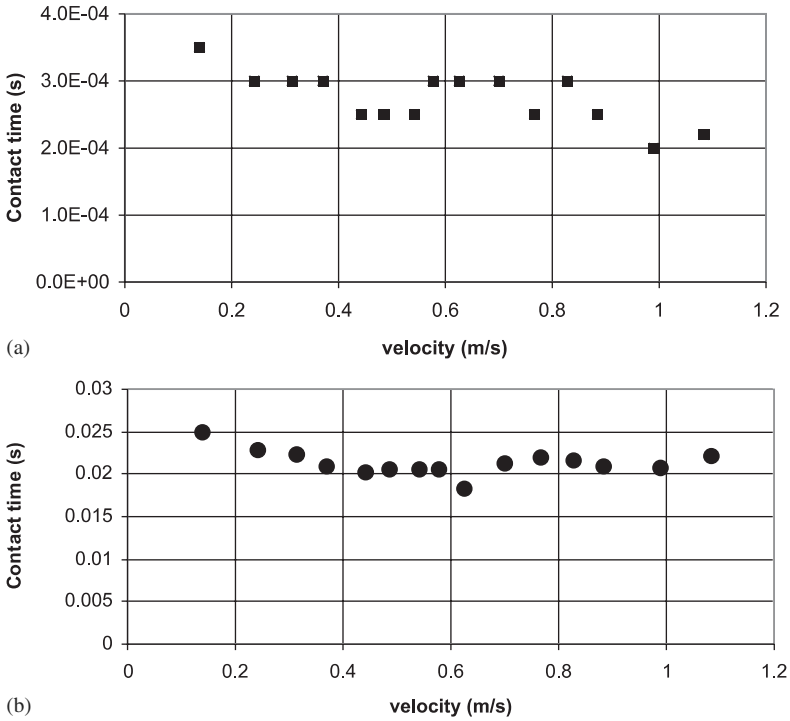

Figure 3. Variation in contact time with velocity for (a) steel on aluminium alloy and (b) steel on sponge buffer material (buffer 1).

the BID $T_c = 0.025$ s. Substituting these values of e and T_c into Equations (9) and (10), the parameters of spring–damper model are found to be $c_b = 530$ N s/m and $k_b = 11.9 \times 10^3$ kN/m for the conventional impact damper and $c_b = 4.05$ N s/m and $k_b = 1.65$ kN/m for the BID, as shown in Table I.

For the simulated response using the two models of impact, the numerical scheme used to integrate the equations of motion was based on the high precision direct scheme of Zhong and Williams [10]. To allow the impact damper to be incorporated into the system, the method was modified to allow non-linear systems to be dealt with [11]. Providing that the time step used is small enough to pick up collisions between the impact mass and the stops, the method is very accurate and it is assumed that discrepancies due to the numerical technique itself are negligible.

3.1. Free vibration response with conventional impact damper

Both experiments and simulations with the impulse–momentum and the spring–damper model were first performed using a conventional impact damper (i.e. without a buffer) to control the response of the SDOF shear frame structure subject to free vibration. An initial lateral displacement of 15 mm was applied to the mass M. The results of the simulation using the impulse–momentum model of impact and the experiment are shown in Figure 4(a). It can be seen that the simulated acceleration response matches the experimental acceleration response well, other than not producing high acceleration peaks at the moments of collision (it should be noted that the

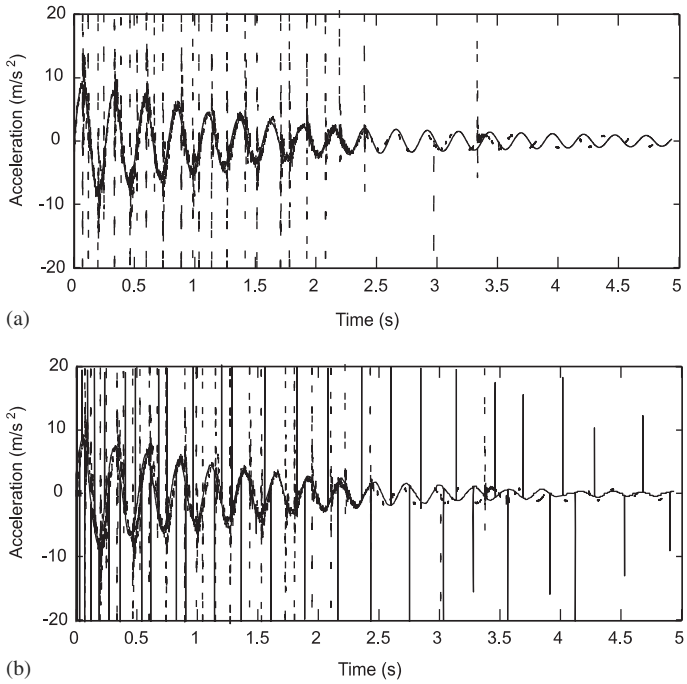

Figure 4. Acceleration time history of free vibration response with conventional impact damper, comparison with experimental results (dotted line) for (a) impulse–momentum simulation (solid line) and (b) spring–damper simulation (solid line).

acceleration peaks from the experimental results are, in most cases, greater than the indicated $\pm 24\,\mathrm{m/s^2}$ but were clipped by limitations in the analogue-to-digital conversion process). The acceleration time history of the simulation result, using the spring–damper model of impact, compared with the experimental result is shown in Figure 4(b). It can be seen that the simulated acceleration record matches the experimental accelerations well. Acceleration peaks similar to those found in the experiment can also be observed in the simulated acceleration response (and, as expected, begin with large amplitude spikes, decreasing as the structural response decreases).

Figure 5 shows the comparison of the power spectral densities (PSDs) of the acceleration response for the experiment (dotted line), the impulse–momentum simulation (dashed line), and the spring–damper simulation (solid line). All three PSDs are very close. It can be concluded that, generally speaking, for the case of a conventional impact damper, the simulation using either the impulse–momentum model or spring–damper model of impact matches the experimental result well, other than the ability of the impulse–momentum model to simulate acceleration peaks caused by collisions.

3.2. Free vibration response with BID

The same test was repeated with the BID. The comparison between experimental results and the results of the simulation using the impulse–momentum model of impact is shown in Figure 6(a). Here, the simulation does not match the experimental result well. This is unsurprising since, with

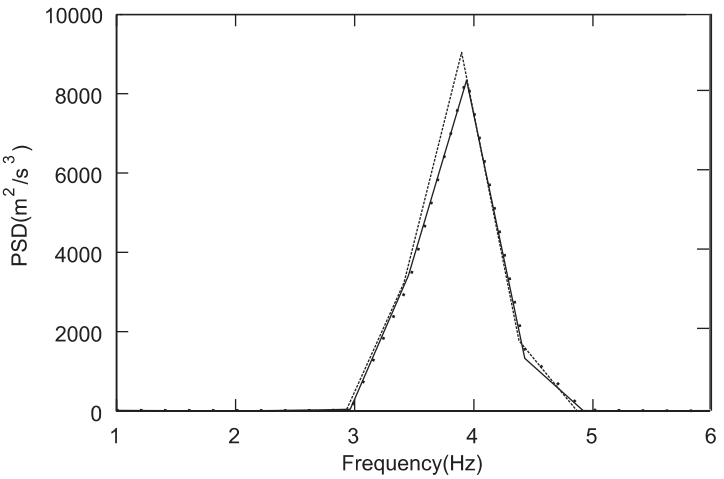

Figure 5. PSD of free vibration response with conventional impact damper, comparison between experimental results (dotted line), impulse–momentum simulation (dashed line), and spring–damper simulation (solid line).

the buffer, the measured contact time of impact is approximately two orders of magnitude greater than that for the conventional impact damper and is not negligible as the impulse–momentum model assumes.

The results of the simulation using the spring–damper model compared with the experimental results are shown in Figure 6(b). Here, the simulated and experimental acceleration responses match well. The acceleration spikes caused by collisions, seen as peaks on the decaying sine curve, can be clearly identified from both the simulation and the experiment and are of similar magnitude and duration.

Figure 7 compares the PSDs of the experimental and simulation responses. While there is a large discrepancy for the impulse–momentum model, the spring–damper model matches experimental results very well. This clearly shows that, when contact time is not negligible, the spring–damper model of impact is more appropriate than the impulse–momentum model.

3.3. Forced vibration response with conventional impact damper

Tests on the same SDOF structure have been carried out under forced vibration, produced using band-limited random base excitation (between 0 and 15 Hz, encompassing the natural frequency of the structure) using a shaking table. The results of the simulation using the impulse–momentum model compared with the experimental results, both with a conventional impact damper, are shown in Figure 8(a). As for the free vibration case, the simulation matches the experimental results reasonably well but, again, without direct simulation of the acceleration spikes representing impacts. Note that the experimentally observed acceleration peaks due to impacts have been truncated in the figure due to scaling of the y-axis. Also, the first two seconds of motion have no impacts and hence are not presented.

The results of the simulation using spring–damper model and experiment are shown in Figure 8(b). The simulation matches the experiment to a similar accuracy as for the

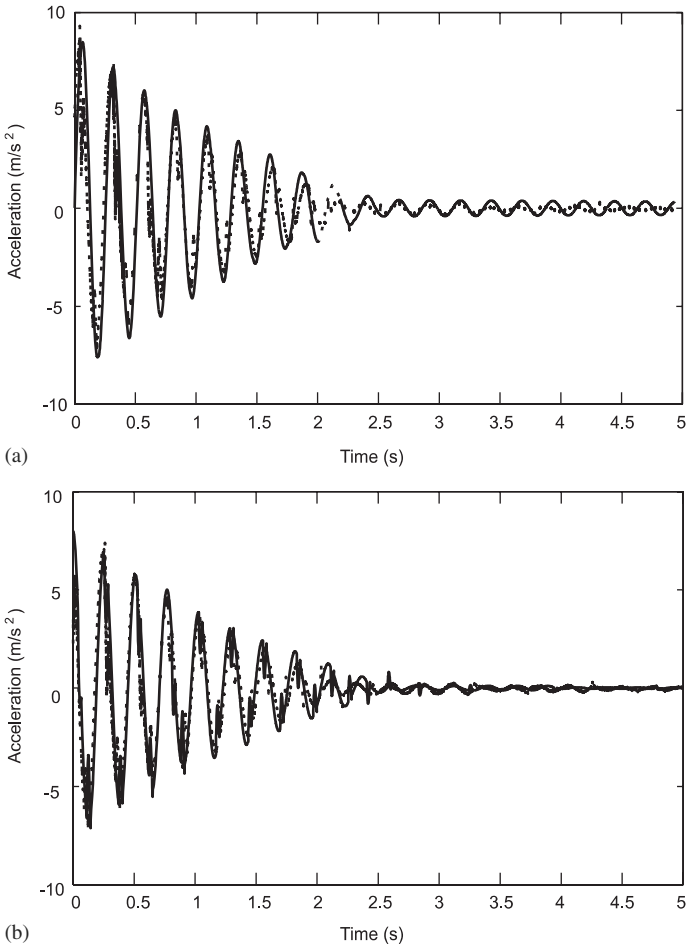

Figure 6. Acceleration time history of free vibration response with buffered impact damper, comparison with experimental results (dotted line) for (a) impulse–momentum simulation (solid line) and (b) spring–damper simulation (solid line).

impulse–momentum model, but peaks caused by collisions are simulated and are of a similar level to those which occurred in the experiment. The PSDs of the experimental and simulated responses are shown in Figure 9, and it can be seen that all three match reasonably well, in particular, at the natural frequency.

3.4. Forced vibration response with BID

The results of the simulation using the impulse–momentum model compared with the experimental results for a BID are shown in Figure 10(a). A significant difference between the results can be observed. The results of the simulation using the spring–damper model of impact are presented in Figure 10(b). This simulation matches the experimental results well. This is particularly evident in the PSD plots, shown in Figure 11, in comparison with the

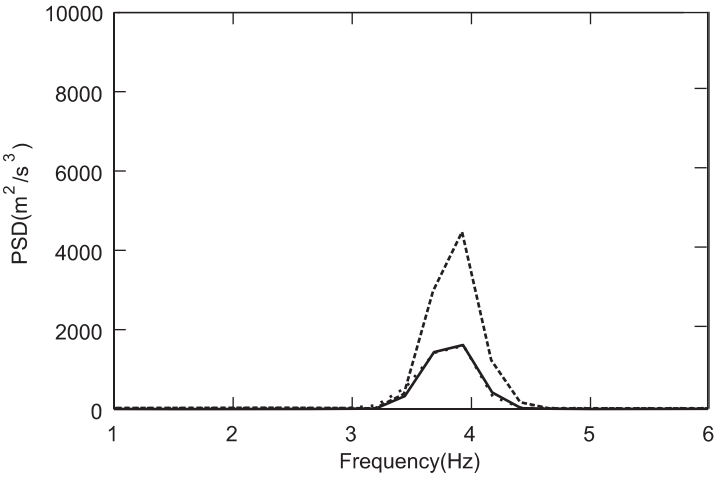

Figure 7. PSD of free vibration response with buffered impact damper, comparison between experimental results (dotted line), impulse–momentum simulation (dashed line), and spring–damper simulation (solid line).

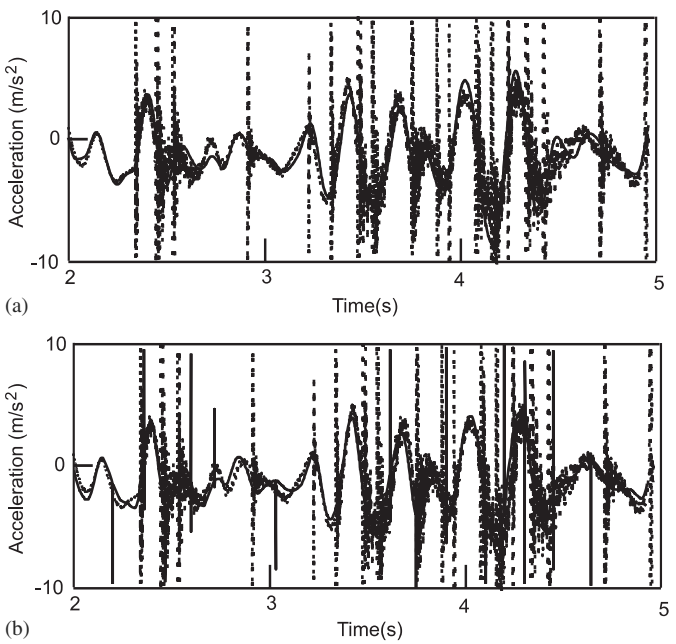

Figure 8. Acceleration time history of forced vibration response with conventional impact damper, comparison with experimental results (dotted line) for (a) impulse–momentum simulation (solid line) and (b) spring–damper simulation (solid line).

impulse–momentum simulation model. These results seem to confirm the results of the free vibration tests, i.e. when the contact is not instantaneous, the impulse–momentum model performs poorly, whereas the spring–damper model performs well.

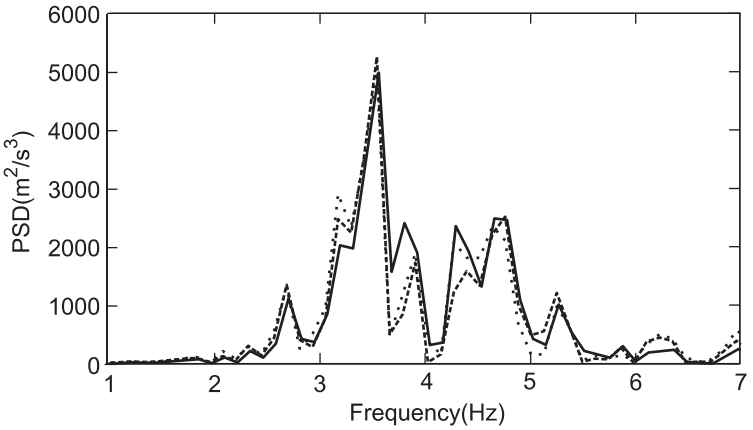

Figure 9. PSD of forced vibration response with conventional impact damper, comparison between experimental results (dotted line), impulse–momentum simulation (dashed line), and spring–damper simulation (solid line).

4. CONTACT FORCE

The experiments described in the previous sections show that the impact model represents the impact behaviour well, in terms of overall behaviour. Further tests were performed in order to investigate how well the spring–damper model represents the actual impact force. In this case, constant amplitude 1 Hz sinusoidal base excitation was applied to the system. Force transducers were used to measure the impact force at the stops. The time history plots for a single impact measured at one of the stops for both the conventional impact damper and the BID are shown by the dotted lines in Figures 12(a) and (b), respectively. As can be seen, the contact force for the BID is two orders of magnitude smaller than that of the conventional impact damper, but the contact time is two orders of magnitude greater. Numerical simulations of the same system, using the stiffness and damping parameters calculated as described in the preceding sections for the appropriate impact bodies, were also carried out, and the resulting simulated impact force is shown by the solid line in Figures 12(a) and (b). In both cases, the simulated impact force profile matches the experimental results very well. This should be unsurprising given that the impact accelerations were simulated well by the spring–damper model. Thus, the spring–damper model is also capable of simulating the actual contact force, unlike the impulse–momentum model. This is significant when it comes to the design of impact dampers where contact force and possible localized damage are important. Similarly, impact accelerations may be important in the design process, for which the spring–damper model can provide information.

5. SENSITIVITY OF THE SPRING–DAMPER MODEL TO MEASURING ERROR OF PARAMETERS

Since both the parameters required for establishing the spring–damper model, k_b and c_b, are calculated from experimentally determined contact time T_c and coefficient of restitution e, the

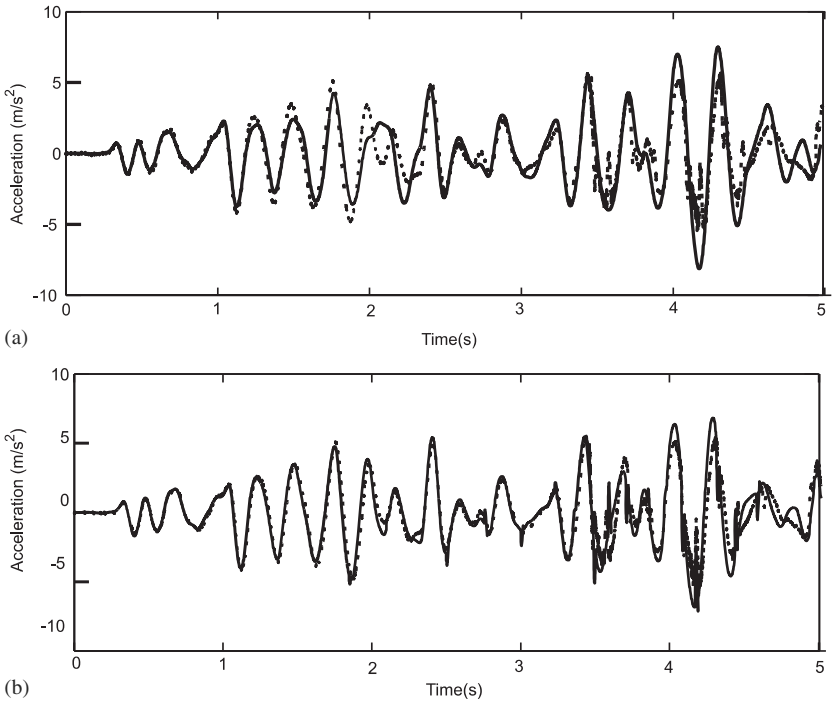

Figure 10. Acceleration time history of forced vibration response with buffered impact damper, comparison with experimental results (dotted line) for (a) impulse–momentum simulation (solid line) and (b) spring–damper simulation (solid line).

sensitivity of the model parameters to measurement errors is examined. From Equations (9) and (10), the sensitivity of k_b and c_b to errors in contact time, ΔT_c, and coefficient of restitution, Δe, can be obtained as follows:

$$s_{k_b}^{e} = \frac{\Delta k_b}{k_b} = \frac{2 \ln e}{(\pi^2 + (\ln e)^2)} \cdot \frac{\Delta e}{e}$$

$$s_{k_b}^{T_c} = -\frac{2\Delta T_c}{T_c}$$

$$s_{c_b}^{e} = \frac{\Delta c_b}{c_b} = \frac{1}{\ln e} \cdot \frac{\Delta e}{e}$$

$$s_{c_b}^{T_c} = -\frac{\Delta T_c}{T_c}$$

It can be seen that measurement errors in T_c and e will not dramatically amplify the model parameters. Figure 13 compares the simulated acceleration response and contacted force with

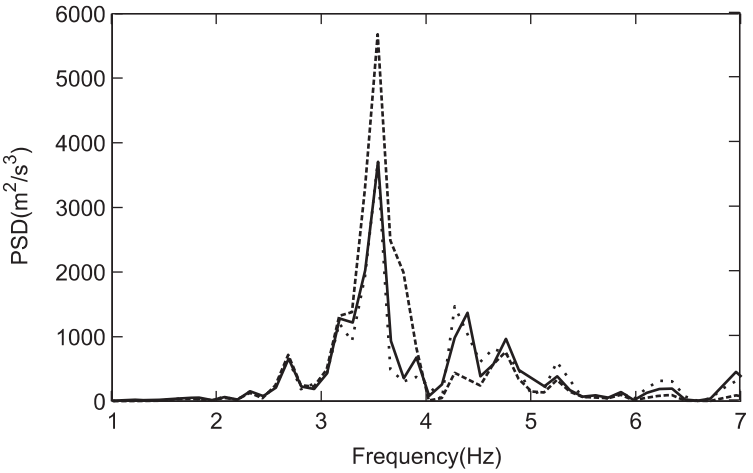

Figure 11. PSD of forced vibration response with buffered impact damper, comparison between experimental results (dotted line), impulse–momentum simulation (dashed line), and spring–damper simulation (solid line).

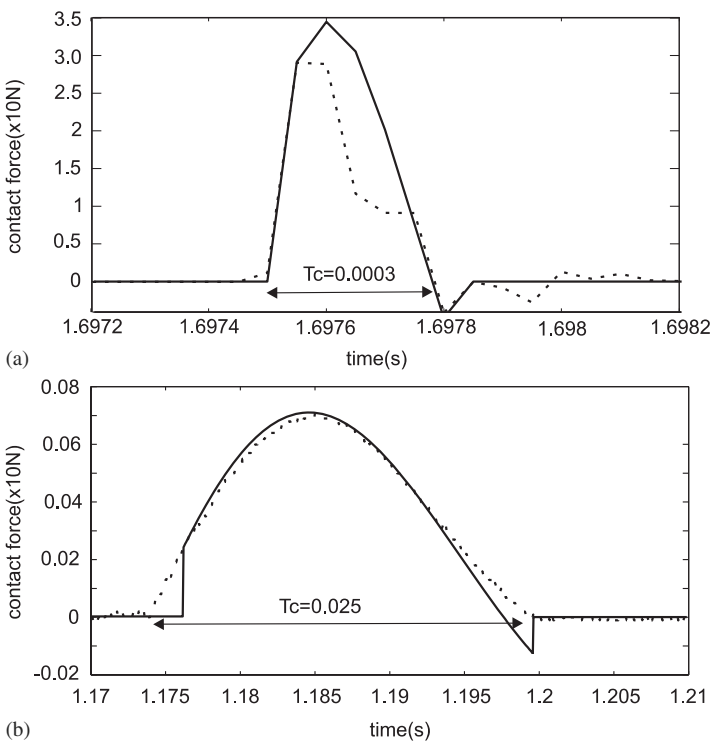

Figure 12. Impact force, comparison between experimental results, and spring–damper simulation for (a) a conventional impact damper and (b) a buffered impact damper.

'exact' values $T_c = 0.025$ and $e = 0.61$ (solid line) and with 10% error in T_c and 15% error in e, i.e. $T_c = 0.0275$ and $e = 0.5185$ (dashed line). It can be seen that the sensitivity of the spring–damper model to the measured parameters is acceptable. This also suggests that a small degree of non-linearity in the measured values (neglected in tests presented earlier) has little effect on the overall response.

6. CONCLUSIONS

Modelling an impact surface using a spring–damper pair is a potentially attractive method of modelling an impact process. However, there are difficulties in defining the spring stiffness and damping parameters, since they do not correspond directly to material properties under high rates of loading. This paper has presented a viable method for deriving these parameters using two more easily measured parameters, i.e. contact time and coefficient of restitution.

The spring–damper model has advantages over other methods for modelling impact, such as the impulse–momentum model, since it directly models the impact process itself, in terms of elastic deformation, energy loss, contact time, and contact force. For impacts occurring between two essentially rigid bodies, such as two steel objects, both an impulse–momentum model and the spring–damper model have been shown to model overall behaviour with sufficient accuracy

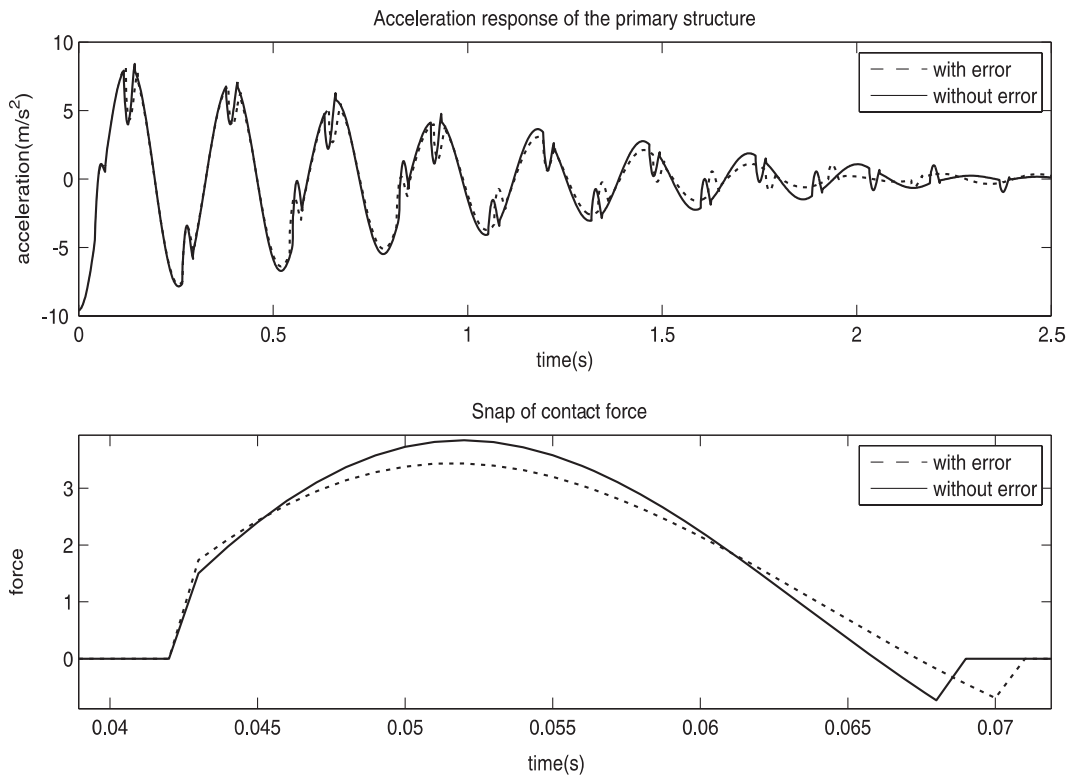

Figure 13. Sensitivity of the model to the parameter error.

for many engineering applications. However, for more elastic impacts, such as the case of a BID, modelling using the impulse–momentum model results in significant error, whereas the spring–damper model, with properly defined parameters, produces results that match observed results well. These conclusions are substantiated by comparison of the two models of impact with test results for a structure under free vibration and more complex forced vibration.

Only in cases where both the deformation of bodies during impact and the contact time are negligibly small can the impulse–momentum model produce acceptable results. The spring–damper model of impact, on the other hand, can take both the elastic deformation and the contact time of impact into consideration, despite the fact that in defining the spring and damper parameters, it too makes use of the coefficient of restitution, albeit indirectly. It can be used to very effectively model impacts of both rigid and elastic bodies macroscopically, provided the contact time and coefficient of restitution can be measured.

NOMENCLATURE

C	damping of SDOF test structure
K	stiffness of SDOF test structure
M	mass of SDOF test structure
T_c	contact time of impact
X_0	initial displacement of SDOF test structure
c_b	damping of contact surface
d	total clearance between impact mass and stops
e	coefficient of restitution
k_b	stiffness of contact surface
m	mass of impact mass
m_i	mass of impact body I
t	time
x_i	displacement of ith mass
$\dot{x}_i$	velocity of ith mass
$\ddot{x}_i$	acceleration of ith mass
y	relative displacement between masses
$\dot{y}_i$	relative velocity between masses
$\dot{y}_0$	initial relative velocity between masses
$\ddot{y}_i$	relative acceleration between masses
μ	mass ratio of two impacting bodies
ω	damped natural frequency
ω_n	undamped natural frequency
ξ	damping ratio of test structure
ζ	damping ratio impact model

ACKNOWLEDGEMENTS

The authors gratefully acknowledge the financial support of the Engineering and Physical Sciences Research Council, Grant No. GR/R15252/01, for the work presented in this paper.

REFERENCES

1. Li K, Darby AP. An experimental investigation into the use of a buffered impact damper. *Journal of Sound and Vibration* 2006; **291**:844–860.
2. Warburton GB. On the theory of the acceleration damper. *Journal of Applied Mechanics* 1957; **24**:322–324.
3. Babat CN. Periodic motion of an impact oscillator. *Journal of Sound and Vibration* 1998; **209**:43–60.
4. Gugan D. Inelastic collision and the Hertz theory of impact. *American Journal of Physics* 2000; **68**:920–924.
5. Masri SF. Forced vibration of a class of non-linear two-degree-of-freedom oscillators. *International Journal of Non-Linear Mechanics* 1972; **4**:663–674.
6. Walton OR. Particle-dynamics calculation of shear flow. *Mechanics of Granular Materials*: *New Models and Constitutive Relations. Proceedings of the US–Japan Seminar on New Models and Constitutive Relations in the Mechanics of Granular Materials*, Ithaca, NY, 22 August 1983. Elsevier: Amsterdam, 1983; 327–338.
7. Cochran AJ. Development and use of one-dimensional model of a golf ball. *Journal of Sports Science* 2002; **20**: 635–641.
8. Fandrich M. Modelling non-destructive impacts macroscopically. *Journal of Mathematical and Computational Modelling* 1998; **28**:205–224.
9. Chatterjee S, Mallik AK, Ghosh A. Impact dampers for controlling self-excited oscillation. *Journal of Sound and Vibration* 1996; **193**:1003–1014.
10. Zhong W, Williams FW. A high precision direct integration scheme for structures subject to transient dynamic loading. *Journal of Computers and Structures* 1995; **56**:113–120.
11. Li K, Darby AP. A high precision direct integration scheme for non-linear dynamic systems. *Journal of Computational Methods in Sciences and Engineering* 2007; submitted for publication.